Modeling and Miniaturization of the Thermoacoustically Driven IPTR to Encourage Sustainable Energy

Mahdi Lavari*

December 2, 2019

Abstract

The Thermoacoustic Stirling Heat Engine(TASHE) designed by Backhaus, a device without moving parts which operates at a frequency of 85 Hz with an average pressure of 3 MPa that is capable of using sustainable energies, is applied to run an Inertance Pulse Tube Refrigerator(IPTR) with 1 W cooling power at 90 K. The coupling of these devices caused to eliminate all moving parts as well as miniaturizing the refrigerator to use for cooling superconducting magnets for MRI systems. A new method for the design of the IPTR performed by using numerical simulation of REGEN3.3. Moreover, to have a better vision of the overall configuration of IPTR and verify the Results of REGEN3.3, DeltaEC is used as an auxiliary software. Fortunately, both software results matched perfectly, and the performance of the IPTR was acoustically and thermodynamically ideal.

Keywords: Thermoacoustics, Inertance Pulse Tube Refrigerator, REGEN3.3, DeltaEC, Sustainable Energy.

1 Introduction

Since the introduction of thermoacoustic technology, cooling below 120 K temperature without moving parts hasn't been a dream. There are many applications in which cryogenic refrigerators are part of the system like liquefaction of oxygen for storage at hospitals and home use, storage of biological cells and specimens, etc [1]. These cryogenic refrigerators utilize thermodynamic cycle concepts that can divide into recuperative (steady flow) and regenerative (oscillating flow) [2]. The Stirling, Gifford-MacMaihan, and Pulse-Tube are different types of the regenerative cryogenic refrigerator. These refrigerators usually are run by compressors that impose moving parts to the system and decrease reliability. However, the introduction of the Thermoacoustic Stirling Heat Engine (TASHE) by Backhaus and Swift [3] let to run a regenerative cryogenic refrigerator with a significant advantage; the system wasn't more than some welded tubes and heat exchangers. The coupling of the Orifice Pulse Tube Refrigerator(OPTR) with the TASHE makes it a suitable match to eliminate every

*Sharif University of Technology. Azadi Ave, Tehran,Iran. Mahdi.lavari@alum.sharif.ir.

moving part to encourage more reliability, less complicity of construction, fewer frequency interferences, etc. The TASHE also can be supplied with various sources of sustainable energy like wasted heated from power plants or solar energy. But, the TASHE-OPTR solution mentioned above doesn't apply to the cases that the refrigerator needs to miniaturize for superconducting applications. So as well as eliminating moving parts, it needs to pay attention to the decreasing size of the refrigerator.

The IPTR works thermodynamically in the Stirling cycle was firstly patented by Robert Stirling [4] in 1816 as the Stirling heat engine. Hershel introduced this cycle as a refrigerator in 1834 [5]. In 1861, Hershel's concept became practical by Alexander Kirk [6].In 1946, Philips Company [7] liquefied air by using the Reverse Stirling Engine. In 1963, Gifford and Longsworth [8] caused major advance by introducing a refrigeration device that worked without displacer at the cold part of the Stirling refrigerator that nowadays is called the Basic Pulse Tube Refrigerator(BPTR). In 1984, an orifice was placed inside the pulse tube by Mikulin et al. [9].A year later, Radebaugh et al. [10] moved this orifice out of pulse tube at its warm end caused the orifice to work as a flow impedance and, as a result, a temperature of 60 K achieved by using Helium gas. This pulse tube arrangement consists of the regenerator, pulse tube, orifice and the reservoir alongside the heat exchangers (see Figure 1) that now referred to as the Orifice Pulse Tube Refrigerator(OPTR).

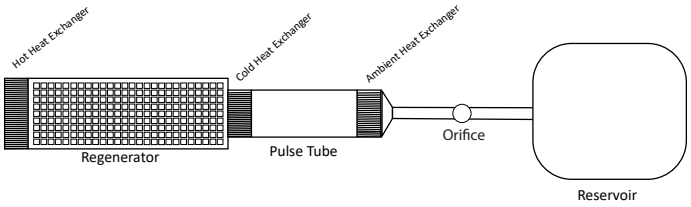

Figure 1: General arrangement of an OPTR

Later studies on developing OPTR led to the discovery of the Inertance tube. In 1996, Godshalk et al. [11] obtained a beneficial phase shift caused by the Inertance tube. This component was simply a long and narrow tube that produced favorable impedance modification in the OPTR. In 1998, Roach and Kashani [12] examined a comparison between the refrigerators with an orifice and Inertance tubes. The results indicated that the Inertance tubes yield dramatic improvements over the use of orifice. In 2000, Marquardt and Radebaugh [13] practiced an Inertance tube in the pulse tube refrigerator to achieve a cooling power of 19 W at 90 K. In 2008, Vanapalli [14] analyzed operation and various aspects of miniaturization of the IPTR. He increased the frequency of the system to decrease the whole volume of the IPTR and studied the effects of the different geometrical and acoustical parameters on the efficiency of the IPTR to minimize various losses. The regenerator geometry was the stainless steel screen with the cold end at 80 K and the warm end at 300 K. The average pressure, pressure ratio at the cold end and the frequency of operation were 3.5 MPa, 1.3 and 120 Hz respectively. In 2017, Srikanth and et al. [15] designed an IPTR that delivered 1 W cooling at 80 K and 100 Hz Frequency.

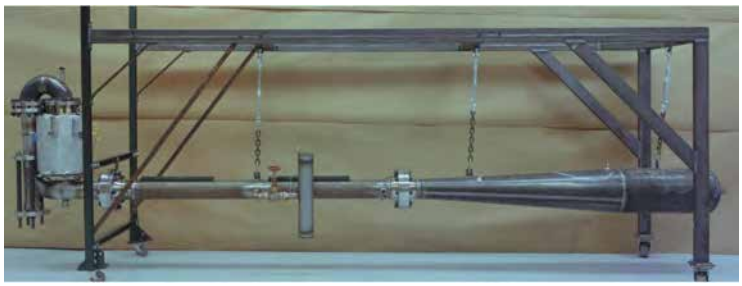

Figure 2: The Thermoacoustic Stirling Heat Engine(TASHE) [22]

Although the TASHE and the IPTR organized on the same phenomenon, called thermoacoustic technology, the TASHE had elapsed through different histories. To study thermoacoustic technology, knowledge of the history of the TASHE is inevitable. Thermoacoustics is the conversion between heat energy and acoustic energy. Thermoacoustics can be divided into the thermoacoustic engine (acoustic power generator) and thermoacoustic refrigerator (acoustic power consumer). According to this classification, the TASHE is a thermoacoustic engine and the IPTR is a thermoacoustic refrigerator. Thermoacoustic systems acoustically consist of standing-wave systems and traveling-wave systems. from the acoustical aspect, 90° differences between pressure phase and velocity phase is called standing-wave and traveling-wave means pressure oscillation is in phase with velocity oscillation.

To follow thermoacoustic history, Byron Higgins [16] in 1777 accidentally discovered that acoustic oscillation occurred in certain positions of the flame in the tube. Moreover, in certain lengths of the fuel supply line, oscillations occurred and could be heard. Sondhauss tube, a tube with one end closed and the other open, was the first thermoacoustic effect studied by Sondhauss in 1850 [17]. In 1959, Rijke [18] installed a well-heated screen in a tube and observed severe acoustic oscillation. This Sondhauss and Rijke tubes regarded as the ancestors of standing-wave and traveling-wave thermoacoustic machines, respectively [19]. Further development achieved by Carter and et al. [20] in 1962. They placed the stack in Sondhauss tube to increase the area for heat transfer. Their thermoacoustic engine produced 27 W acoustic Power from 600 W power input.In 1979, Ceperley [21] offered a type of thermoacoustic engine was different from the Sondhauss tube. Miraculously he observed the motion and pressure cycles of the gas in the regenerator of a normal Stirling engine are identical with those occurring in the regenerator of a traveling-wave heat engine. It is now known as a traveling-wave Stirling engine [1]. Ceperley's concept wasn't practical until 1999, Backhaus and Swift designed and fabricated a novel traveling-wave thermoacoustic engine, which is known as a Thermoacoustic Stirling Heat Engine(TASHE). The TASHE achieved 42% of Carnot efficiency which is comparable to that of a traditional engine [3]. The world's first TASHE shown in Figure 2 worked at above 80 Hz frequency [22].

About 10 years before the introduction of the TASHE, in 1990, Swift and Radebaugh [1] developed a pulse tube refrigerator run by a thermoacoustic standing-wave engine. This thermoacoustically driven pulse tube refrigerator (TADPTR) led to a refrigeration temperature of 90 K with an operating fre-

Figure 3: Prototype of acoustic liquifier(TASHE-OPTRs) [23]

quency of 40 Hz. In 2000, Los Alamos National Laboratory(LANL) and PRAXIER revised the TASHE as the driver, instead of an original standing-wave thermoacoustic engine that used in TADPTR [24]. This thermoacoustic system worked with helium at an average pressure of 450 psi, with oscillations up to 45 psi in amplitude at a frequency of 40 Hz [25]. The major thermoacoustic subsystems were an engine to generate high-intensity acoustic power from high-temperature heat, a wave tube to transport the acoustic power from the engine to the refrigerators and to determine the 40 Hz operating frequency and three refrigerators to generate useful cryogenic refrigeration while consuming the acoustic power. These three pulse tube refrigerators were designed with regenerators of 20 cm diameter and pulse tubes of 10 cm diameter [26].

Modifying the frequency of the world's first TASHE to 40 Hz in TASHE-OPTR, provoked an increase in the volume of the whole configuration and made it a bulky system. the discrepancy of these two types of TASHE size is obvious by comparison between Figure 2 and Figure 3. The frequency of the world's first TASHE is changed to provide a good match with a typical Pulse Tube Refrigerator worked with 40 Hz frequency. Until recently. The poor heat transfer and high pressure-drop losses in the regenerative heat exchanger at frequencies above 60 Hz performed an obstacle to gain efficient operation of regenerative refrigerators. In 2006, Radebaugh and O'Gallaher [27] noticed that the right combination of frequency and pressure, along with optimized regenerator geometry, can lead to efficient regenerator operation at a frequency much above 60 Hz. By raising the frequency of pulse tube, the rational result is the miniaturization of the whole system and improving the intensity of the output because of the increasing of oscillating mass flow.

As a gap found in the literature review, the design of the Inertance Pulse Tube Refrigerator run by the first world's TASHE (with operation frequency above 80 Hz) can be a good candidate to gain advantages like miniaturization of the system along with no moving parts, mechanical vibration-free, using of sustainable energies, etc. The approach for modeling and analysis in this paper

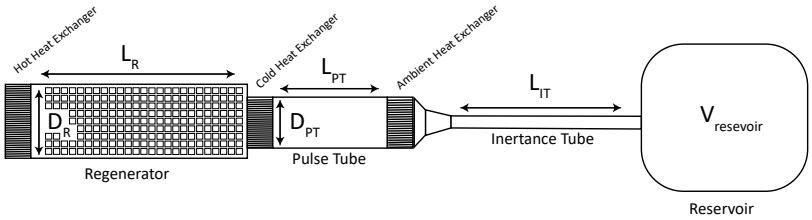

Figure 4: General arrangement of a typical inline IPTR

mostly conducted by numerical simulation. So 1-D models, DeltaEC by LANL and REGEN3.3, have been used to design a unique miniaturized refrigerator system driven by the first world's TASHE. The system that is discussed is referred to as the Inertance Pulse Tube Refrigerator(IPTR) and produces a cooling power of 1.0 W at 90 K and 85 Hz.

2 The Inertance Pulse Tube Refrigerator

The IPTR is a Stirling-type refrigerator that works with an oscillating pressure where the amplitude of oscillation is typically about 10% to 30% of the average pressure. The average pressure is in the range of 1 to 3 MPa and frequencies are in the range of 20 to 60 Hz [1]. Helium is normally used as the working fluid because of its ideal gas properties, high thermal conductivity, and high ratio of specific heats.

In an ideal IPTR with an isothermal regenerator and an adiabatic pulse tube, the process is reversible. Consequently, the COP of the refrigerators has a maximum called the COP of Carnot of the refrigerator. It is given by Equation 1 [28] but the COP of the cooler reduced by the dissipated energy.

$$\mathrm{COP}_{\mathrm{Carnot}} = \frac{T_{\mathrm{h}}}{T_{\mathrm{c}} - T_{\mathrm{h}}} \tag{1}$$

Here T_{h} is the temperature of the hot end of the regenerator, T_{c} temperature of the cold end of the regenerator. Since the design of ideally operating IPTR is determined by deeply understanding the function and operation principle of its components. The IPTR includes four major components consists of the regenerator heat exchanger, pulse tube, inertance tube, and reservoir. These components presented in Figure 4.

2.1 Regenerator

The IPTR is a regenerative refrigerator. This classification is because of the existence of at least one regenerator heat exchanger that operates with the oscillating flow. The regenerator consists of a pile of stainless-steel screens. The regenerator is sandwiched by cold and hot heat exchangers, therefore, maintains

a smooth temperature profile between the two adjacent heat exchangers.

The function of the regenerator is to act as a heat storage tank. While hot gas passed through the porous medium of the regenerator, heat absorbed by the heat capacity of the matrix for a half cycle. In backward mode, the cold gas flowing in the opposite direction picked up the heat from the matrix and returned the matrix to its original temperature before the cycle repeated. As a result, these heat exchanges transmit acoustic power or PV power of the driver, here the TASHE, to the cold end of the regenerator of the IPTR with a minimum of loss. The time-averaged acoustic power [29] transmits through the regenerator is given by:

$$\langle \dot{W} \rangle_t = \langle \boldsymbol{P}\, \dot{\boldsymbol{V}} \rangle_t = (1/2)\, |\boldsymbol{P}||\, \dot{\boldsymbol{V}}\, | \cos\theta. \tag{2}$$

Where the bold symbols represent time-varying or phasor variables, such as pressure $\boldsymbol{P}$, volume flow rate $\dot{\boldsymbol{V}}$. The phase angle θ is the phase between pressure and flow.

Most losses of the IPTR happen in the regenerator. These losses consist of thermal ineffectiveness (enthalpy flow), pressure drop and thermal conduction. These losses are functions of the dimensions and operation parameters of the regenerator. Vanapalli [14] analyzed the regenerator losses and determine the variation of losses with specific area and length of the regenerator. He discovered that to have lower fractional void volume losses, the specific area and the length should be smaller which, is conflicting with the pressure drop and heat transfer losses (specific area should be larger for lower losses) and conduction loss (length should be larger for lower loss). The optimum specific area is a tradeoff between pressure drop, enthalpy flow, conduction, and void volume losses. Radebaugh and O'Gallagher [27] also suggested much smaller hydraulic diameters regenerator material and smaller regenerator volumes at high pressures required for the high-frequency operation of the regenerator and reduction of losses.

2.2 Pulse Tube

The IPTR operates ideally with adiabatic compression and expansion in the pulse tube, therefore it should insulate the processes at its two ends. Besides, it must be long enough that gas flowing from the warm end traverses only partway through the pulse tube before the flow reversed, so the gas parcels that flow in from one side of the pulse tube never reach another side. With these criteria, gas in the middle portion of the pulse-tube never leaves the pulse-tube and forms a temperature gradient that insulates the two ends. This middle portion gases act like a displacer in Stirling-type refrigerator. Turbulence in the pulse-tube must be avoided due to its effect on the insulation of the two ends.

2.3 Inertance Tube

The inertance effect mechanism has developed to cause a beneficial phase shift between the flow and the pressure at the warm end of the pulse tube. These mechanisms have led to improved efficiencies in the pulse tube refrigerators. An Inertance tube can be placed at the warm end of the pulse tube to have a proper phase of mass flow with respect to the pressure in the regenerator.

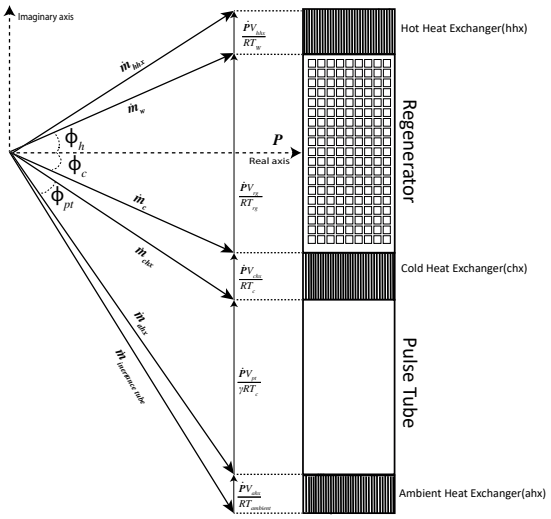

Figure 5: The phasor diagram of an IPTR

Radebaugh [30] pointed out the correct phasing occurs when the mass flow or the volume flow through the regenerator is approximately in phase with pressure.

The phasor diagram (see Figure 5) of the regenerator and pulse tube indicates they have a similar effect on the phase angle between pressure and flow. When gas flows due to rising pressure from the driver to reservoir volume, so it passes through the regenerator, pulse tube. Both the regenerator and the pulse tube caused the flow phase to lead the pressure phase similarly. Radebaugh and et al. [29] learned to achieve optimum phase angle of flow lagging pressure by about 30° at the cold end means that the Inertance tube will need to lag the flow at its inlet by about 60° to accommodate the change in phase through the pulse tube.

2.4 Reservoir Volume

The function of reservoir volume is to be large enough that the effect of pressure can be omitted despite oscillating flow occurs.

3 The TASHE

The TASHE is shown in Figure 6, is an example of a traveling-wave refrigerator. The TASHE provides one way to achieve the required acoustic work to drive the IPTR. The TASHE produces acoustic power while the gas in the regenerator experiences thermal expansion when the pressure is high and thermal contraction when the pressure is low. Therefore each cycle occurred generates the acoustic waves and makes them more strength. Like the IPTR, if the regenerator of the TASHE is in a suitable acoustic network, the flow along the regenerator's temperature gradient is in phase with the pressure, so good thermal contact between gas and regenerator is required to cause the thermal expansion and contraction steps to be in phase with the oscillating pressure.

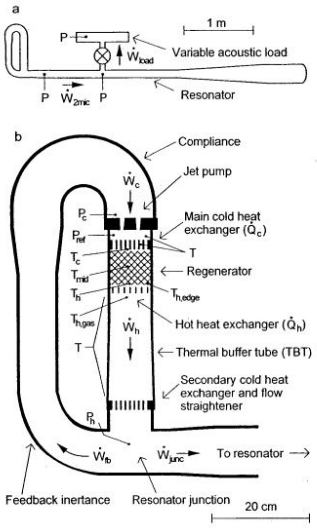

Figure 6: Schematic cross-section of the Backhaus-Swift thermoacoustic-Stirling engine. (a) is the arrangement of TASHE that consists of the looped acoustical network shown in (b) and a standing-wave resonator [31].

The first's world TASHE (see Figure 6) is a 30 bar helium filled the system, oscillating at 85 Hz. The resonator was essentially half-wavelength, with pressure oscillations 180° out of phase at the right end of the fat portion on the right and in the small torus containing the heat exchangers on the left. The highest velocity occurred in the center of the resonator, at the small end of the long cone. The highest pressure amplitude occurred in the ambient heat exchanger [22].

4 Numerical Simulation of the IPTR

The approaches for design and analysis of the IPTR mostly conducted by numerical simulation. Base on this fact, the modeling of IPTR investigated by REGEN3.3 and DeltaEC. DeltaEC has a one-dimensional approach and treats a thermoacoustic model as a series of standardized segments. DeltaEC performs simultaneous integrations along x of the conservation equations of momentum, continuity, and energy. Its equations are modified by using sinusoidal parameters and takes advantage of practical parameters to include losses like pressure drops. REGEN3.3 integrates with respect to both x and t but makes no restrictive assumption that the time dependence must be periodic.

4.1 DeltaEC

In 1868, Kirchhoff calculated acoustic attenuation in a duct due to oscillatory heat transfer between the solid isothermal duct wall and the gas sustaining the sound wave [20]. In 1969-1983, Rott et al. [19] established a sound theoretical foundation applicable to both thermoacoustic prime mover and heat pumps. In 2001, Swift wrote a book and presented a simplified form of governing equation

for acoustics waves under "Rott's acoustic approximation" [22]. The main idea was to apply sinusoidal terms of pressure, temperature, and density to the conservation law of mass, momentum, and energy and neglecting the second-order involving the product of two small value terms in equations. These equations represent a set of linear and time-dependent equations that can found in swift's book. Ward and Swift [32] developed a program for thermoacoustic computation base on numerical integration of Rott's acoustic approximation. This software is now named Design Environment for Low-amplitude thermoacoustic Engines Conversion(DeltaEC) [33].

DeltaEC deals with one spatial dimension sequence of thermoacoustic elements called segments. It integrates momentum and continuity equations that include additional effects such as dissipation of acoustic power along the sides of the geometry chosen by the user such as ducts, compliances, transducers, and thermoacoustic stacks and regenerators. It uses different equations in different segments to suit local circumstances but typical types of equations that used as momentum and continuity equations [34] are given by:

$$\frac{dp_1}{dx} = -\frac{i\omega\rho_m}{A}U_1, \tag{3}$$

$$\frac{dU_1}{dx} = -\frac{i\omega A}{\rho_m a^2}p_1. \tag{4}$$

Where A is an cross-sectional area, p_1 pressure amplitude, U_1 volume flow rate, a sound speed, ρ_m mean density, ω angular frequency. The Equation 3 is derived from the momentum equation of fluid mechanics and the Equation 4 is derived from the continuity equation of fluid mechanics.

DeltaEC assuming that oscillatory flow losses can be calculated by using the steady-flow Moody friction factor at each instant of time during the oscillatory flow, A turbulence algorithm can be enabled in DUCT and CONE, which specify the relative roughness (roughness height divided by pipe diameter).

DeltaEC uses a shooting method, by guessing and adjusting any unknown boundary conditions at the initial segment to achieve desired boundary conditions elsewhere. The user of DeltaEC enjoys considerable freedom in choosing which variables used as boundary conditions and which computed as part of the solution. With its multi-parameter shooting method to satisfy a variety of mixed boundary conditions, DeltaEC gives the user considerable freedom in choosing which variables are computed as solutions. So it is obvious that any corrupt and impractical inputs as boundary condition caused outputs converges to wrong and impractical answers. In this paper, the literature review used to consider practical inputs for DeltaEC.

4.2 REGEN3.3

The first version of REGEN was distributed by the National Institute of Standards and Technology(NIST) as REGEN3.1 in 1989 [35]. This software was revised and distributed as REGEN3.2 and REGEN3.3. The numerical approximation of REGEN is a discretization of the differential equations for the conservation of mass, momentum, and energy in the gas and regenerator matrix. The result is a nonlinear system of equations for the temperature, pressure and mass flux at all the mesh points simultaneously is solved by a Newton iteration.

The program finds the solution to the conservation equations that satisfy the input conditions.

In REGEN3.3, losses associated with regenerator ineffectiveness (enthalpy flow), conduction through the matrix, and pressure drop calculated by the model. The optimization process through the use of REGEN3.3 conducted by altering the oscillation frequency and temperatures of both ends of the regenerator to set an optimum specific area of the regenerator.

5 Design Process

This section describes a systematic design procedure of an IPTR operating around 90 K temperature with 1 W cooling. The design method starts with defining inputs and requirements. The primary parameters of interest for an IPTR are cooling power, operating temperature, average and dynamic pressure, and frequency. Because the TASHE, as the driver, imposed fixed inputs on the IPTR, the measures of merit should be considered to choose a suitable segment from the DeltaEC model of the TASHE from reference [34].

5.1 Input from the TASHE

The TASHE consists of various segments that shown in Figure 7 from the DeltaEC model of the TASHE with different values of acoustic power and phase angle between flow and pressure. The TASHE-OPTR designed by LANL and PRAXIER used the resonator segment of the TASHE as output for the OPTR shown in Figure 8a and Figure 8b. This segment is a standing-wave segment because the phase relation between flow and pressure is above 60°. As a result, the phase relation needed to be adjusted to pursue a favorable input for the OPTR. This reason indicated that adjustment of the first world's TASHE was necessary to fit correctly with the efficient OPTR to minimize losses. To join an IPTR with the first world's TASHE, some measures of merit evaluated from the literature review to make a suitable effect on the design of the IPTR. They listed as follows:

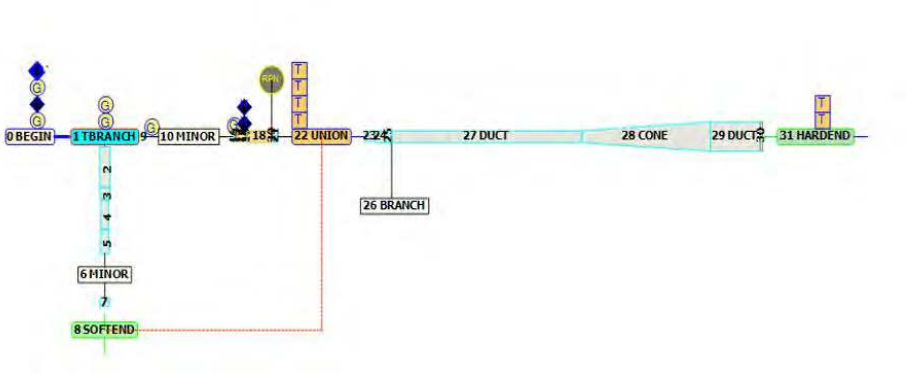

Figure 7: DeltaEC model of the TASHE

1. Flow phase should lead pressure phase more as possible at the cold end of

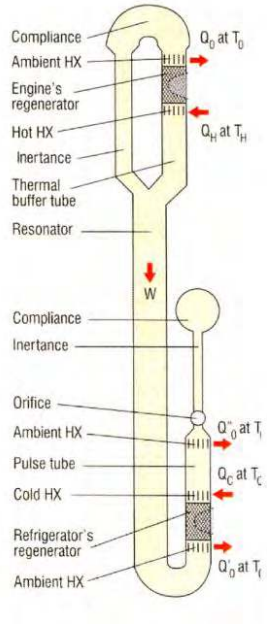

(a) The schematic of the TASHE-OPTR [25]

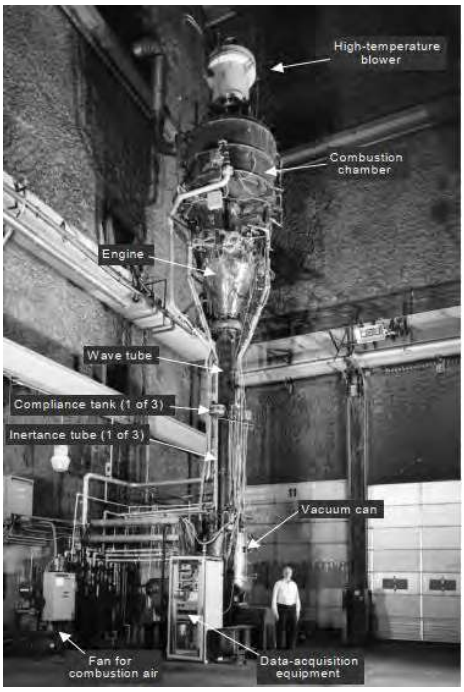

(b) The TASHE-OPTR [26]

Figure 8: The TASHE-OPTR

regenerator to have pressure and flow in phase in the midpoint of regenerator [14].

2. More acoustic power means more refrigeration power.

3. Higher pressure ratio is a better choice but this should not exceed 1.5 because above this value, the equations can't assume linear anymore and the low-amplitude approximation is not valid [22].

4. The inline arrangement of the IPTR (see Figure 4) is the most efficient because it decreases void volume losses [2].

According to these measures of merit, Segment 9 selected as input from the DeltaEC model of the TASHE. Table 1 exhibits its parameters. The pressure ratio, acoustic power and phase relation between flows with pressure perfectly match with desired values.

Table 1: Segment 9 of DeltaEC model of the TASHE

Segment 9 parameters	values
Frequency(Hz)	85
Mean pressure(MPa)	3.1
Temperature hot end of regenerator(K)	325
Amplitude of pressure(MPa)	0.3
Phase of pressure(°)	0
Amplitude of volume flow (m3/s)	0.016
Phase of volume(°)	32
Acoustic power(W)	2009
Pressure ratio	1.21
Phase volume flow leads pressure(°)	32

5.2 Numerical Simulation

After defining inputs and requirements, the approximate configuration of the IPTR should be estimated before running the simulation code to design the IPTR. Since there are too many possible combinations in the selection of geometric parameters such as diameter and length of the regenerator and the pulse tube, using all of the possible combinations in simulation code is not practical. As a starting point, three typical IPTR design parameters that their frequency is within the range 60-120 degree and mean pressure are between 25-35 bars were selected from the literature review shown in Table 2.

Table 2: Three typical design data of the IPTR

Design Parameter	Ref. [30]	Ref. [15]	Red. [14]
Frequency(Hz)	60	100	120
Mean pressure(MPa)	2.5	3.5	3.5
Temperature hot end of regenerator(K)	300	300	300
Temperature cold end of regenerator(K)	80	80	80
Specific area of regenerator(m^2/kg)	0.052	0.058	0.054
Length of regenerator(mm)	52	35	30
Diameter of regenerator(mm)	25.6	7	9.5
COP	0.117	0.1044	0.078
Phase that flow lead pressure at cold end(°)	-39	-30	-30
Pressure ratio	1.3	1.3	1.3
Refrigeration power(W)	25	1	6.1

As shown in Table 2, flow phase angle lead pressure phase angle about 30° and it totally agrees with Radebaugh [29]. Hence -30° phase angle at the cold end of the regenerator used as a fixed parameter in the design of the IPTR. Another parameter is the specific area of the regenerator which is the ratio of the gas cross-sectional area to mass flow at the cold end. Vanapalli [14] investigated that the value specific area in miniaturization of the IPTR played a big role in the efficiency of overall IPTR. As shown in Table 2, $0.054 m^2/kg$,the

average of values in Table 2, used as an initial value for the specific area value in REGEN3.3. The pressure ratio (the ratio of the maximum pressure to the minimum pressure) is directly related to the intensity of the acoustic wave. unfortunately, the TASHE imposed 1.21 as the pressure ratio on the IPTR.

After specifying defined cooling power (1 W), operating temperature (90 K), average pressure (3.1 MPa), dynamic pressure (0.3 MPa), and frequency (85 Hz). A model of the IPTR with input from the TASHE developed by DeltaEC along with a series of run carried out by REGEN3.3 to determine the size of the regenerator and maximizing the COP of the regenerator. The Figure 9 represents segments of the IPTR that modeled by DeltaEC. Segments in Figure 9 from left to right are the regenerator (No.4), pulse tube (No.9), inertance tube (No.11) and reservoir volume (No.12).

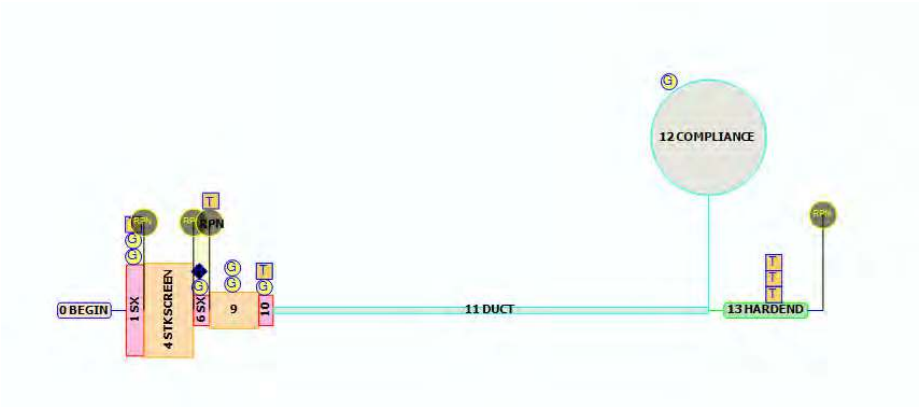

Figure 9: The IPTR modeled by DeltaEC

6 Result

To design a regenerator that can perform 1 W of cooling at 90 K, REGEN3.3 performed using an iterative optimization process. Initial guesses made with respect to the regenerator length, regenerator inner diameter and an optimal phase shift (between pressure and velocity) at the cold end of the regenerator. Simultaneously, initial guesses for configuration of the IPTR obtained from references were used to set up a series of run on DeltaEC. The efforts were made to bring DeltaEC and REGEN3.3 outputs closer together as same as maximum COP was the target.

6.1 REGEN3.3

Many runs were applied by REGEN3.3 to configure regenerator until maximum COP reached. Results from the final run result shown in Table 3.

Table 3: Regenerator parameters derived from REGEN3.3

Parameter	Values
Frequency(Hz)	85
Mean pressure(MPa)	3.1
Refrigeration power (W)	1
Temperature of hot end of regenerator(K)	325
Temperature of cold end of regenerator(K)	90
Phase that flow lead pressure at cold end(°)	-28
Acoustic power at hot end of regenerator (W)	-1917
Acoustic power at hot end of regenerator (W)	549
COP	0.121
Material of regenerator	Stainless steel
Porosity of regenerator	0.6939
Hydraulic diameter of regenerator(μm)	44.88
Working fluid	Helium
Diameter of regenerator(m)	0.08
Length of regenerator(m)	0.05

6.2 DeltaEC

Different configurations of the IPTR with input from the TASHE tested by DeltaEC by changing different segments of DeltaEC. The result can found in Table 4. The primary 3-D model of the designed IPTR depicted in Figure 10.

Table 4: The IPTR parameters derived from DeltaEC

Design Parameter	Values
Frequency(Hz)	85
Mean pressure(MPa)	3.1
Refrigeration power(W)	1
Temperature hot end of regenerator(K)	325
Temperature cold end of regenerator(K)	90
Acoustic power at hot end of regenerator (W)	-1959
Acoustic power at cold end of regenerator (W)	519
Diameter of regenerator(m)	0.08
Length of regenerator(m)	0.05
Diameter of pulse tube(m)	0.04
Length of pulse tube(m)	0.055
Diameter of inertance tube(m)	0.006
Length of inertance tube(m)	0.05
Volume of reservoir(m^3)	0.0011

7 Performance of the IPTR

The regenerator works isothermally and the pulse tube works adiabatically in an ideal IPTR. Figure 11 originated by DeltaEC, represents the temperature gradient over the IPTR length. As shown in Figure 11, temperature profile

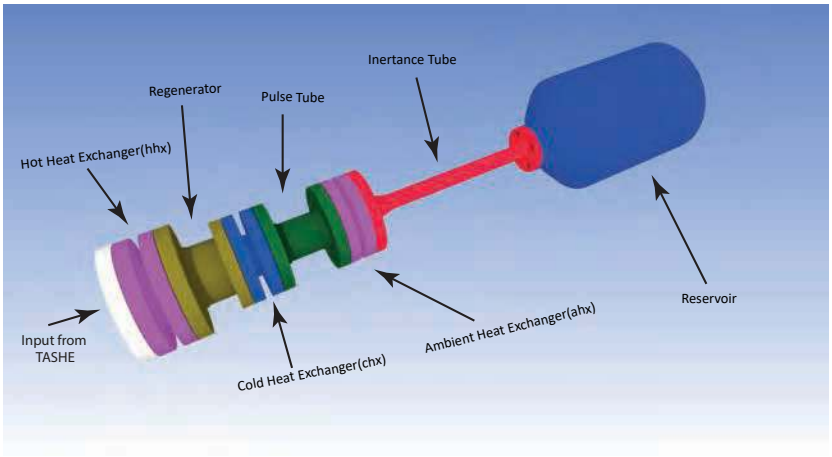

Figure 10: The 3-D model of the IPTR

dropped (from Segment 1 to segment 4) from 325 K with a linear slope to 90 k over regenerator length. This linear slope indicates that the regenerator is isothermal. It means that heat exchange between gas parcels and porous media in the regenerator is perfect and at any surface of it, the temperature is constant. The temperature profile (from segment 5 to segment 9) displays temperature raised from 90 K to 300K with a nearly nonlinear slope due to the adiabatic background of the pulse tube. The rest segments include the inertance tube and the reservoir experienced 300 K (ambient) temperature.

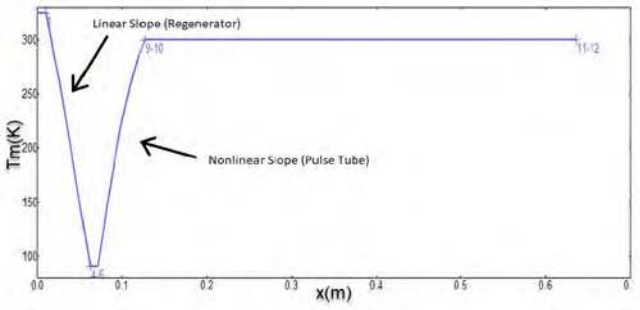

Figure 11: Temperature gradient over length of the IPTR from DeltaEC

To evaluate the IPTR from the acoustical viewpoint, the amplitude of pressure over the IPTR length proves the nature of sinusoidal waves inside the refrigerator. Figure 12 attests that the amplitude of pressure along IPTR follows one-quarter of the cosine function. It seems the IPTR perfectly managed from an acoustical perspective.

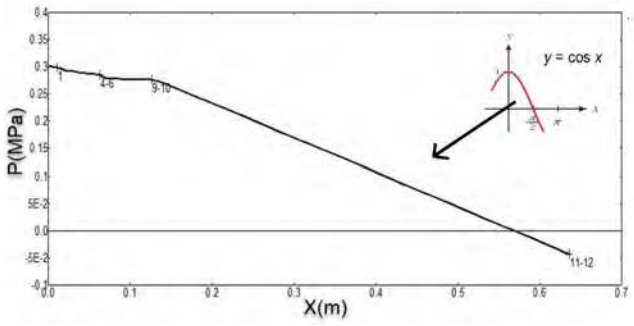

Figure 12: Amplitude of pressure over length of the IPTR from DeltaEC

Figure 13 is the amount of acoustic power over the length of the IPTR. Figure 13 explains that the regenerator is the most important component of the IPTR due to its massive consumption of acoustic power (from segment 1 to segment 4). So by optimizing the regenerator, the acoustic power that remains at the cold end of the regenerator can be increased for a fixed input acoustic power. It is noteworthy to pay attention that the left acoustic power consumed by the inertance tube (from segment 10 to segment 11) to provide a suitable phase shift in the IPTR.

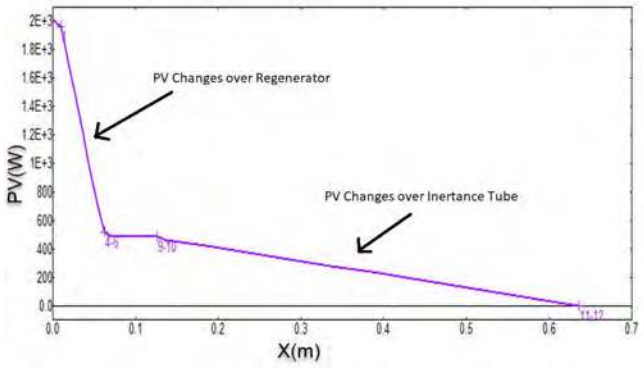

Figure 13: Acoustic power over length of the IPTR from DeltaEC

8 Verification of the IPTR Model

To judge and further verify the validity of the design made by REGEN3.3 and DeltaEC, their results compared. The acoustic power at the cold and hot end of the regenerator is evaluated by both software is shown on Table 5. the smallest differences between outputs of REGEN3.3 and DeltaEC represents that two models perfectly matched with each other. REGEN3.3 and DeltaEC calculate equations with different assumptions. For REGEN3.3, losses associated with regenerator ineffectiveness (enthalpy flow), conduction through the matrix, and pressure drop are computed by the model and conduction loss through the tube wall containing the regenerator material is calculated separately. However, DeltaEC utilized some practical factors to calculate losses. Therefore, these

percentages of discrepancy mean that the dominant losses of both models set with minimum values.

Table 5: The acoustic power at both end of regenerator

Parameter	REGEN3.3	DeltaEC	Difference
Acoustic powers at hot end(W)	-1917	-1959	2.1%
Acoustic powers at cold end(W)	549	519	5.7%

Another important graph between outputs of REGEN3.3 to verify the validity and convergent of the results on the model is the conservation of energy in the regenerator. The total energy should be equal to the sum of the heat conduction and the enthalpy flow. From Figure 14, the convergence of the numerical solution can be perceived as well as satisfying the first law of thermodynamics. The energy flow at any cross-section of the regenerator must be equal to the sum of enthalpy flow and heat conduction. So, Figure 14 confirms that the conservation of energy along regenerator length is constant.

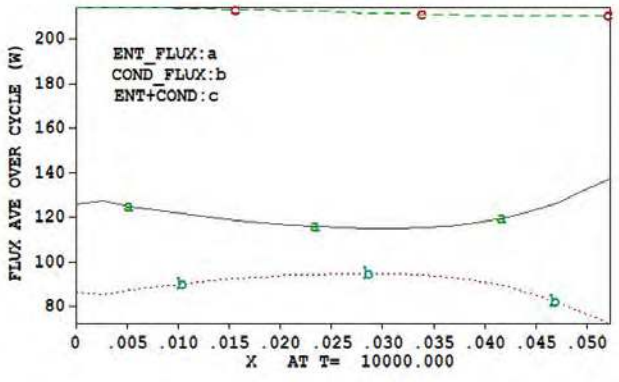

Figure 14: The conservation of energy in the regenerator

9 Conclusion

This paper dealt with investigating a method to design an Inertance Pulse Tube Refrigerator to be driven by the TASHE. The literature review showed that high-frequency operation of the IPTR with acceptable efficiency is available. Two separate models by DeltaEC and REGEN3.3 was considered to design the IPTR. Inputs, constraints, and measures of merit derived from the literature review and the DeltaEC model of the TASHE. Both REGEN3.3 and DeltaEC models approximately shared similar results due to the diminishing of losses on both models. The results of Models indicated that the IPTR with 1 W cooling at 85 Hz and 90 K was available with reasonable efficiency. Performance study of the IPTR exhibited that the pressure amplitude was cosine function and the regenerate and pulse tube worked isothermally and adiabatically, respectively. Finally, the verification of models evaluated by the conversion of energy and comparison between the two model results.

References

[1] R. Radebaugh, "Development of the pulse tube refrigerator as an efficient and reliable cryocooler," Proceedings of the Institute of Refrigeration, vol. 96, 01 2000.

[2] R. Radebaugh, "Pulse tube cryocoolers for cooling infrared sensors," in Infrared Technology and Applications XXVI (B. F. Andresen, G. F. Fulop, and M. Strojnik, eds.), vol. 4130, pp. 363 – 379, International Society for Optics and Photonics, SPIE, 2000.

[3] S. Backhaus and G. W. Swift, "A thermoacoustic stirling heat engine," Nature, vol. 399, pp. 335–338, 05 1999.

[4] G. T. Reader, "Stirling regenerators," Heat Transfer Engineering, vol. 15, no. 2, pp. 19–25, 1994.

[5] R. Radebaugh, Low Temperature and Cryogenic Refrigeration, vol. 99, ch. Pulse Tube Cryocoolers, pp. 415–434. Springer, Dordrecht, 2003.

[6] A. C. KIRK, "On the mechanical production of cold. (includes plates and appendix," Minutes of the Proceedings of the Institution of Civil Engineers, vol. 37, no. 1874, pp. 244–315, 1874.

[7] J. Köhler and C. Jonkers, "Fundamentals of the gas refrigeration machine," Philips Tech. Rev, vol. 16, no. 3, pp. 69–78, 1954.

[8] W. E. Gifford and R. C. Longsworth, "Pulse-tube refrigeration," Journal of Engineering for Industry, vol. 86, pp. 264–268, 08 1964.

[9] E. I. Mikulin, A. A. Tarasov, and M. P. Shkrebyonock, Low-Temperature Expansion Pulse Tubes, pp. 629–637. Boston, MA: Springer US, 1984.

[10] R. Radebaugh, J. Zimmerman, D. R. Smith, and B. Louie, A Comparison of Three Types of Pulse Tube Refrigerators: New Methods for Reaching 60K, pp. 779–789. Boston, MA: Springer US, 1986.

[11] K. M. Godshalk, C. Jin, Y. K. Kwong, E. L. Hershberg, G. W. Swift, and R. Radebaugh, Characterization of 350 Hz Thermoacoustic Driven Orifice Pulse Tube Refrigerator with Measurements of the Phase of the Mass Flow and Pressure, pp. 1411–1418. Boston, MA: Springer US, 1996.

[12] P. R. Roach and A. Kashani, Pulse Tube Coolers with an Inertance Tube: Theory, Modeling, and Practice, pp. 1895–1902. Boston, MA: Springer US, 1998.

[13] E. Marquardt and R. Radebaugh, "Pulse tube oxygen liquefier," Adv. Cryo. Eng., vol. 45, 01 2000.

[14] S. Vanapalli, High-frequency Operation and Miniaturization aspects of Pulse-tube Cryocoolers. PhD thesis, University of Twente, Netherlands, 3 2008. 10.3990/1.9789036526524.

[15] T. Srikanth, Padmanabhan, C. S. Gurudath, A. Amrit, S. Basavaraj, and K. Dinesh, "Design of high frequency pulse tube cryocooler for on-board space applications," IOP Conference Series: Materials Science and Engineering, vol. 171, p. 012081, feb 2017.

[16] A. A. Putnam and W. R. Dennis, "Survey of organ-pipe oscillations in combustion systems," The Journal of the Acoustical Society of America, vol. 28, no. 2, pp. 246–259, 1956.

[17] K. Feldman, "Review of the literature on sondhauss thermoacoustic phenomena," Journal of Sound and Vibration, vol. 7, no. 1, pp. 71 – 82, 1968.

[18] K. Feldman, "Review of the literature on rijke thermoacoustic phenomena," Journal of Sound and Vibration, vol. 7, no. 1, pp. 83 – 89, 1968.

[19] G. Chen, K. Tang, and T. Jin, "Advances in thermoacoustic engine and its application to pulse tube refrigeration," Chinese Science Bulletin, vol. 49, pp. 1319–1328, Jul 2004.

[20] G. W. Swift, "Thermoacoustic engines," The Journal of the Acoustical Society of America, vol. 84, no. 4, pp. 1145–1180, 1988.

[21] P. H. Ceperley, "A pistonless stirling engine—the traveling wave heat engine," The Journal of the Acoustical Society of America, vol. 66, no. 5, pp. 1508–1513, 1979.

[22] G. Swift, Thermoacoustics: A unifying perspective for some engines and refrigerators. 01 2001.

[23] G. Swift and J. Wollan, "Thermoacoustics for liquefaction of natural gas," GasTIPS, vol. 8, pp. 21–26, 01 2002.

[24] B. Arman, J. Wollan, G. Swift, and S. Backhaus, "Thermoacoustic natural gas liquefiers and recent developments," Proceedings of the 2003 International Conference on Cryogenics and Refrigeration, pp. 123–127, 01 2003.

[25] G. Swift and J. Wollan, "Thermoacoustics for liquefaction of natural gas," GasTIPS, vol. 8, pp. 21–26, 01 2002.

[26] B. Arman, J. Wollan, V. Kotsubo, S. Backhaus, and G. Swift, "Operation of thermoacoustic stirling heat engine driven large multiple pulse tube refrigerators," in Cryocoolers 13 (R. G. Ross, ed.), (Boston, MA), pp. 181–188, Springer US, 2005.

[27] R. Radebaugh and A. O'Gallagher, "Regenerator operation at very high frequencies for microcryocoolers," AIP Conference Proceedings, vol. 823, pp. 1919–1928, 04 2006.

[28] A. T. A. M. de Waele, "Basic operation of cryocoolers and related thermal machines," Journal of Low Temperature Physics, vol. 164, 09 2011.

[29] R. Radebaugh, M. Lewis, E. Luo, J. M. Pfotenhauer, G. F. Nellis, and L. A. Schunk, "Inertance tube optimization for pulse tube refrigerators," AIP Conference Proceedings, vol. 823, no. 1, pp. 59–67, 2006.

[30] J. Pfotenhauer, Z. Gan, and R. Radebaugh, "Approximate design method for single stage pulse tube refrigerators," AIP Conference Proceedings, vol. 985, pp. 1437–1444, 03 2008.

[31] S. Backhaus and G. W. Swift, "A thermoacoustic-stirling heat engine: Detailed study," The Journal of the Acoustical Society of America, vol. 107, no. 6, pp. 3148–3166, 2000.

[32] W. C. Ward and G. W. Swift, "Design environment for low-amplitude thermoacoustic engines," The Journal of the Acoustical Society of America, vol. 95, no. 6, pp. 3671–3672, 1994.

[33] J. Clark, W. Ward, and G. Swift, "Design environment for low-amplitude thermoacoustic energy conversion," Journal of The Acoustical Society of America - J ACOUST SOC AMER, vol. 122, 11 2007.

[34] B. Ward, J. Clark, and G. Swift, Users Guide: Design Environment for Low-amplitude Thermoacoustic Energy Conversion DeltaEC. Los Alamos National Laboratory, version 6.4b2 ed., 6 2016.

[35] J. Gary and A. O'Gallagher, REGEN3.3: USER MANUAL. National Institute of Standards and Technology, 4 2008.